

Creep analysis of an earth embankment on soft soil deposit with and without PVD improvement

Rezania, M., Bagheri, M., Mousavi Nezhad, M. & Sivasithamparam, N.

Author post-print (accepted) deposited by Coventry University's Repository

Original citation & hyperlink:

Rezania, M, Bagheri, M, Mousavi Nezhad, M & Sivasithamparam, N 2017, 'Creep analysis of an earth embankment on soft soil deposit with and without PVD improvement' *Geotextiles & Geomembranes*, vol. 45, no. 5, pp. 537-547.

<https://dx.doi.org/10.1016/j.geotexmem.2017.07.004>

DOI 10.1016/j.geotexmem.2017.07.004

ISSN 0266-1144

Publisher: Elsevier

NOTICE: this is the author's version of a work that was accepted for publication in *Geotextiles & Geomembranes*. Changes resulting from the publishing process, such as peer review, editing, corrections, structural formatting, and other quality control mechanisms may not be reflected in this document. Changes may have been made to this work since it was submitted for publication. A definitive version was subsequently published in [*Geotextiles & Geomembranes*, [45], [5], (2017)]
DOI: 10.1016/j.geotexmem.2017.07.004

© 2017, Elsevier. Licensed under the Creative Commons Attribution-NonCommercial-NoDerivatives 4.0 International

<http://creativecommons.org/licenses/by-nc-nd/4.0/>

Copyright © and Moral Rights are retained by the author(s) and/ or other copyright owners. A copy can be downloaded for personal non-commercial research or study, without prior permission or charge. This item cannot be reproduced or quoted extensively from without first obtaining permission in writing from the copyright holder(s). The content must not be changed in any way or sold commercially in any format or medium without the formal permission of the copyright holders.

This document is the author's post-print version, incorporating any revisions agreed during the peer-review process. Some differences between the published version and this version may remain and you are advised to consult the published version if you wish to cite from it.

Creep analysis of an earth embankment on a soft soil deposit with and without PVD improvement

Mohammad Rezania^{a,*1}, Meghdad Bagheri^{b,2}, Mohaddeseh Mousavi Nezhad^{a,3},
Nallathamby Sivasithamparam^{c,4}

^aSchool of Engineering, University of Warwick, Coventry, UK

^bDepartment of Civil Engineering, University of Nottingham, Nottingham, UK

^cComputational Geomechanics Division, Norwegian Geotechnical Institute, Oslo, Norway

Abstract

In this paper, an anisotropic creep constitutive model, namely Creep-SCLAY1S is employed to study the installation effects of prefabricated vertical drains (PVDs) on the behavior of a full scale test embankment, namely Haarajoki embankment in Finland. Half of the embankment is constructed on unimproved natural soft soil while its other half is constructed on the PVD improved soil foundation. The Creep constitutive model, used in this study, incorporates the effects of fabric anisotropy, structure and time within a critical state based framework. For comparison, the isotropic modified Cam clay (MCC) model and the rate-independent anisotropic S-CLAY1S model are also used for the analyses. The results of the numerical analyses are compared with the field measurements. Based on the results it is found that the creep model provides an improved approximation of settlements and excess pore pressure dissipations. In addition, the application of two commonly used permeability matching techniques for two dimensional (2D) plane-strain analysis of the PVD problem is studied and the results are discussed in detail.

^{*},¹Corresponding author. E-mail address: m.rezania@warwick.ac.uk. Tel.: +44 24 76 522339.

² E-mail address: meghdad.bagheri@nottingham.ac.uk. Tel.: +44 115 95 12850.

³ E-mail address: m.mousavi-nezhad@warwick.ac.uk. Tel.: +44 24 765 22332.

⁴ E-mail address: nallathamby.siva@ngi.no. Tel.: +47 406 94 933.

22 **Keywords:** Geosynthetics; Embankment; PVDs; Soft clay; Creep behavior; Advanced
23 constitutive modeling

24 **1 Introduction**

25 In order to tackle the delayed consolidation settlement problem typical of soft soils, installation
26 of prefabricated vertical drains (PVDs), combined with preloading, has become popular in the
27 industry as an effective ground improvement solution (e.g. [Abuel-Naga et al. 2015](#), [Lam et al.](#)
28 [2015](#), [Wang et al. 2016](#)). Preloading is an old way of dealing with the problem of long-term
29 consolidation in soft soils; however, in practice, this procedure on its own can be considerably
30 time consuming. For the excess pore water pressure (PWP) to be dissipated quickly, the
31 drainage paths need to be shortened. PVDs are geosynthetic slender elements made of
32 corrugated plastic cores that their installation can effectively reduce the consolidation time as
33 they provide short horizontal drainage paths in thick soft soil deposits that need improvement
34 ([Rowe and Taechakumthorn 2008](#)).

35 Some aspects of PVD installation e.g., well resistance, smear effect and the overlapping of
36 smear zones have been widely studied (e.g. [Kim and Lee 1997](#), [Zhu and Yin 2000](#), [Cascone](#)
37 [and Biondi 2013](#), [Deng et al. 2013](#), [Xue et al. 2014](#), [Chen et al. 2016](#), [Nguyen and Indraratna](#)
38 [2017](#)). However, very few studies exist regarding the long-term effects of PVD installation on
39 the response of the soft soil layer (e.g. [Kim 2012](#), [Lo et al. 2013](#), [Hu et al. 2014](#)), this deemed
40 to be in part due to the unavailability of appropriate soil models. Many soil constitutive models,
41 which are commonly used for the analysis and design of geotechnical engineering problems,
42 assume that the behavior of soil is simply isotropic. Application of such simplified models in
43 practice often provide solutions that are overly conservative and costly, and in some cases
44 result in uncertainties regarding long-term performances. In reality, the behavior of natural
45 soils is highly anisotropic. Natural clays also have an inherent structural property that gives
46 them an undisturbed shear strength in excess of their remolded strength. Furthermore, clayey
47 soils are known to be the most susceptible to time effects on their strength and deformation
48 characteristics. An accurate prediction of soft soil response, either improved or unimproved,

49 requires that these aspects of their behavior are considered by the employed constitutive
50 model.

51 Because of considerable computational cost of three dimensional (3D) finite element (FE)
52 analysis, the boundary value problems related to PVD ground improvement are commonly
53 modelled in the representative 2D plane-strain condition. However, as the water flow into the
54 PVD is an axisymmetric problem; therefore, for the representative 2D analysis, a number of
55 so-called mathematical matching techniques have been proposed (e.g. [Hird et al. 1992](#), [Lin et
56 al. 2000](#), [Indraratna et al. 2005](#)). These matching methods are used for the conversion of the
57 permeability coefficient from axisymmetric state into plane-strain condition.

58 The aim of this paper is to numerically analyze the long-term effects of PVD installation on the
59 behavior of the improved soft clay deposit, and to verify the accuracy and the consistency of
60 a recently developed creep constitutive model in predicting the consolidation settlements and
61 deformations at a practical level. For this study primarily an advanced creep constitutive
62 model, namely Creep-SCLAY1S ([Sivasithamparam et al. 2015](#)), is used for carrying out the
63 numerical analysis. An instrumented embankment on soft clay, namely Haarajoki test
64 embankment ([Finish National Road Administration, 1997](#)) is simulated. This test embankment
65 is constructed on deep soft soil deposits improved with PVDs for one half of its length. The
66 results from the newly developed creep model are compared with those obtained by using a
67 time-independent anisotropic model, S-CLAY1S ([Karstunen et al. 2005](#)), and the MCC model
68 ([Roscoe and Burland, 1968](#)). In addition, a simple comparative study is carried out in order to
69 examine the sensitivity of the results to the adopted matching technique.

70 **2 Creep-SCLAY1S Model**

71 The Creep-SCLAY1 ([Sivasithamparam et al. 2015](#)) is an extension of S-CLAY1 ([Wheeler et
72 al. 2003](#)) to incorporate rate-dependent response of clays. In this model the elliptical surface
73 of the S-CLAY1 model is adopted as the Normal Consolidation Surface (NCS), i.e. the
74 boundary between small and large irreversible (creep) strains. Furthermore, in this model

75 creep is formulated using the concept of a constant rate of visco-plastic multiplier (Grimstad
76 et al. 2010). The new creep model incorporates the same rotational hardening law as that of
77 the S-CLAY1 and S-CLAY1S models. Moreover, the Creep-SCLAY1 model has been further
78 extended by incorporating the destructuration hardening law of the S-CLAY1S model to take
79 into account the effect of the initial inter-particle bonding in the soil response. Despite
80 assuming anisotropy of plastic behavior, the S-CLAY1 class of models assume isotropy of
81 elastic behavior which is a reasonable assumption for modelling the behavior of soft and
82 sensitive clays (Rezania et al. 2016a). In addition to the soil parameters required for modelling
83 with SCLAY1S (as detailed in Karstunen et al. 2005), the use of Creep-SCLAY1S requires
84 three viscous parameters namely, the reference time, τ , the modified creep index, μ^* , and the
85 intrinsic value of the modified creep index, μ_i^* . Note that μ^* is related to the one-dimensional
86 secondary compression index, C_α , as

$$\mu^* = C_\alpha / [\ln 10 (1 + e_0)] \quad (1)$$

87 The extended Creep-SCLAY1S model has recently been successfully applied for modelling
88 pile installation effects in a soft clay deposits (Rezania et al. 2016b)

89 **3 Numerical modelling of PVD-improved ground**

90 For planning a PVD ground improvement work, penetration depth, installation pattern and
91 spacing of PVDs are the important factors that need to be taken into consideration. For the
92 Haarajoki embankment the length of the PVDs used was 15 m and for simplicity they were
93 installed in a square pattern (Fig. 1a), as opposed to a triangular pattern (Fig. 1b), with a
94 spacing of $S = 1 \text{ m}$. The equivalent diameter, D , is the diameter of soil medium that is
95 discharging water into its corresponding PVD and it is calculated based on the spacing S
96 between the PVDs. For the square pattern $D = 1.128S$.

97 During PVD installation, the insertion and removal of the mandrel modifies the properties of
98 the neighboring soil. This effect mainly concerns the densification and disturbance of soil

99 structure, thus it is known as “smear” effect and the affected zone as “smear zone” (Fig. 1c).
100 The diameter of smear zone, D_s , depends on many factors including size of the mandrel,
101 installation method, the structure of the soil etc. Several studies have been carried out on the
102 determination of D_s (e.g., [Xiao 2001](#)), and its value is often considered to be in the range of 3-
103 5 times the diameter of the mandrel, D_m , or 5-8 times the equivalent drain diameter, D_w .

104 Ideally the study of PVD ground improvement is a 3D problem, requiring a 3D FE analysis.
105 However, such a model would be computationally very expensive. Therefore, often a 2D
106 plane-strain FE model is used and a matching technique is employed to convert the general
107 permeability of the medium into an equivalent plane-strain value. In practice, the axisymmetric
108 unit cell representing a drain is simplified into a plane-strain unit cell, assuming an equivalent
109 half width, B , for the cell.

110 A number of simplified matching approaches are available in the literature which are based
111 on manipulation of, either the drain spacing or the soil permeability. For the simplicity of
112 relationships each drain is assumed to work independently, a constant soil permeability is
113 adopted and consolidation is considered to take place in a uniform soil column with linear
114 compressibility characteristics ([Yildiz et al. 2009](#)). Comparing the numerical results in
115 literature, it seems that the 2D plane-strain analyses do not give a satisfactory agreement in
116 estimating the maximum value of excess pore pressure after construction. This may be
117 because the geometry and/or the permeability of the domain are changed but the
118 compressibility of the soil itself remains constant. Nonetheless, regardless of this issue, the
119 matching technique proposed by [Hird et al. \(1992\)](#) appears to be the most convenient one as
120 it allows the mesh size to be controlled. Another advantage of this technique is that no
121 particular smear zone is required to be considered in the modelling.

122 A simple permeability matching technique has also been proposed by [Lin et al. \(2000\)](#), where
123 matching is done for the horizontal permeability (see Equation (2))

$$k_{hpl} = \frac{k_h \pi}{6 \left[\ln\left(\frac{n}{s}\right) + \frac{k_h}{k_s} \ln(s) - \frac{3}{4} \right]} \quad (2)$$

124 where k_{hpl} is the equivalent horizontal permeability of surrounding soil in plane-strain
 125 condition, k_h is the horizontal permeability of the undisturbed soil, k_s is the horizontal
 126 permeability of the smeared zone, $n = R/R_w$ and $s = R_s/R_w$ where R , R_w and R_s are the radius
 127 of the unit cell (equivalent radius), the drain, and the smear zone, respectively. In this paper
 128 the matching technique proposed by [Hird et al. \(1992\)](#) together with the one proposed by [Lin](#)
 129 [et al. \(2000\)](#) have been used to carry out numerical analyses.

130 The drain adopted at the site was reported to have an average width of 98.7 mm with a
 131 discharge capacity of 157 m³/year. The equivalent diameter of the drain, calculated according
 132 to the formulation proposed by [Hansbo \(1979\)](#) is 67 mm. Considering for the smear effect the
 133 ratios $k_h/k_s = 20$ and $D_s/D_w = 8$, values that proved to give accurate results when used with
 134 the advanced constitutive models of the S-CLAY family ([Yildiz et al. 2009](#)), the equivalent
 135 plane-strain permeability is $k_{hpl} = 0.0126k_h$.

136 The advanced models, S-CLAY1S and Creep-SCLAY1S, have been implemented into the
 137 finite-element code PLAXIS AE ([Brinkgreve et al. 2014](#)) through the user-defined soil model
 138 facility of the software ([Rezania et al. 2014](#)). Details of the simulations carried out, and the
 139 analysis of the results, in comparison with field performances, are discussed in the following.

140 **3.1 Haarajoki embankment**

141 Haarajoki embankment has a height of 2.9 m and a length of 100 m. Its crest is 8 m wide and
 142 the slopes have a gradient of 1:2. It was founded on a 2 m thick dry crust lying above a 20.2 m
 143 thick soft clay deposit. The foundation soil consists of soft soil with a high degree of anisotropy
 144 and some inter-particle bonding. Half of the embankment (50-m-long section) was constructed
 145 on PVD improved soft soil and the other half was built on the natural soft soil without any
 146 ground improvement measure.

147 A finite element mesh with 6-noded triangular elements is used for the FE analyses, with extra
148 degrees of freedom for excess PWP at corner nodes (during consolidation analysis). Mesh
149 sensitivity studies have been done to ensure that the mesh is dense enough to produce
150 accurate results. The geometry of the FE model is shown in Fig. 2; for the model, the far right
151 boundary is assumed at 40 m distance from the centerline. The bottom boundary of the clay
152 deposit is assumed to be completely fixed in both horizontal and vertical directions; whereas,
153 the left and right vertical boundaries are only restrained horizontally. Drainage is allowed at
154 the ground level, while due to unknown hydraulic conditions at the bottom boundary, this
155 boundary is considered impermeable. Impermeable drainage boundaries are also assigned to
156 the lateral boundaries. Based on ground data, the water table is assumed to be at the ground
157 surface. For the side of the embankment that was built on improved soil, PVDs are
158 incorporated in the model using the drain element in PLAXIS. Groundwater head is assumed
159 to be at ground level for all drains.

160 The embankment was built in 0.5m thick layers and each layer was placed and compacted
161 within 2 days, except for the foundation layer which was built within 5 days. For the calculation
162 phases, plastic analyses are carried out corresponding to the construction process of the
163 embankment, after which the consolidation analysis is performed.

164 **3.1.1 Parameters estimation**

165 The embankment itself is modelled using the simple linear elastic-perfectly plastic Mohr-
166 Coulomb model with the following reported values for the embankment material: Young
167 modulus $E = 40000$ kPa, Poisson's coefficient $\nu = 0.35$, cohesion $c' = 2$ kPa, friction angle
168 $\phi' = 40^\circ$, unit weight $\gamma = 21$ kN/m³.

169 For the numerical simulation, the first layer (0-2 m) is divided into two parts; the first sub-layer
170 (0-1 m) is modelled with the Mohr-Coulomb model using $E = 2300$ kPa, $c' = 1$ kPa and
171 $\phi' = 30^\circ$. The second sub-layer (1-2 m) is modelled by assigning the relative advanced soil

172 constitutive model used in the analysis without consideration of the effect of soil structure,
173 given that the soil at this layer has low sensitivity due to being fairly disturbed.

174 Based on the site investigation data and parameter values reported by [Karstunen et al. \(2015\)](#),
175 the soft soil deposit beneath Haarajoki embankment can be sub-divided into seven layers with
176 different parameter values. The values of model constants and state variables used for the
177 different soil layers are summarized in Table 1. In this table the conventional soil constants,
178 such as the elasticity constants κ and ν , and the critical state constants λ , λ_i (i.e., the intrinsic
179 value of λ) and M are the same as those for the MCC model, hence their values are determined
180 in the standard manner. The values of the advanced anisotropic model parameters have been
181 determined following the approaches proposed in [Wheeler et al. \(2003\)](#) (for evaluation of
182 anisotropy parameters α_0 , ω and ω_d), and [Karstunen et al. \(2005\)](#) (for evaluation of
183 destructuration parameters χ_0 , ζ and ζ_d).

184 Variation of permeability k with void ratio e during consolidation analysis is represented in
185 simulations through permeability change index parameter c_k which is calculated according to
186 the following equation proposed by [Berry and Poskitt \(1972\)](#)

$$c_k = \frac{e - e_0}{\log\left(\frac{k}{k_0}\right)} \quad (3)$$

187 The values of the constant c_k can be obtained from the results of the oedometer tests.

188 For evaluation of the creep parameter, μ_i^* , ([Sivasithamparam et al. 2015](#)) the value of creep
189 index, C_α , measured from conventional oedometer test results is used. According to [Mesri and](#)
190 [Godlewski \(1977\)](#), the ratio of C_α/λ can be considered to be constant for each clay layer. The
191 intrinsic value of the creep index $C_{\alpha i}$ (the subscript i stands for the intrinsic values)
192 corresponding to the intrinsic compression index λ_i of each layer can be obtained by $C_{\alpha i}\lambda_i/\lambda$.
193 The values of the μ_i^* are essentially derived using the Equation (1). It should be noted that the
194 value of μ_i^* significantly influences the results, therefore its appropriate calibration is essential

195 for realistic modelling of the long-term behavior. For determination of μ_i^* values based on the
196 abovementioned approach, a number of available laboratory test data were carefully
197 interpreted and the C_α and λ values which provide best simulation results were selected.
198 Finally, the values of modified intrinsic compression and swelling indexes, λ_i^* and κ^* , are
199 obtained as $\lambda_i^* = \lambda_i / (1+e)$ and $\kappa^* = \kappa / (1+e)$ with e being the void ratio (Leoni et al., 2008).
200 Furthermore, Table 2 summarizes the parameter values used for the calculation of the
201 equivalent plane-strain permeability, according to the employed matching technique. The
202 modified coefficients of permeability of the soil layers, k_{hpl} , are presented in Table 3.

203 3.1.2 Results and discussion

204 3.1.2.1 Settlements

205 Fig. 3a shows settlement predictions versus time at the node directly under the centerline of
206 the embankment (point A in Fig. 2) for the side of the embankment that is not improved with
207 PVDs. It can be seen in the figure that the creep model provides an improved prediction of the
208 field measurements, however it is clearly on the conservative side. MCC grossly
209 underestimates the settlements. It is capable to accurately predict the settlement that occurred
210 in early stages; however, the predicted settlement rate slows down after about day 50, pointing
211 out that the model cannot take into consideration the time-dependent aspect of the soil
212 behavior. Application of S-CLAY1S model leads to a similar settlement prediction trend, but,
213 compared to MCC, it provides a less conservative modelling result as it considers the effects
214 of inherent features of natural soil behavior, particularly destructuration (i.e., strain softening).

215 Vertical settlement plots calculated for the side of the embankment built on the PVD improved
216 soil are presented in Fig. 3b. It is observed that all three constitutive models capture the effect
217 of PVD installation on accelerating the settlement of the soft ground. Settlement prediction by
218 the Creep-SCLAY1S model matches well with the field observations. It demonstrates that the
219 model is capable of providing an enhanced simulation for complex scenarios where soil strata
220 consists of both undisturbed and disturbed (smear zone) segments combined with drainage
221 elements.

222 Surface settlement field data is available for the side of the embankment that was built on
223 unimproved soil. The measurements were taken on 10 days, 5 years and 10.7 years after
224 construction. The data has been used to investigate the surface settlement through predictions
225 from different models (see Fig. 4). With regards to the embankment side that was built on the
226 unimproved ground (Fig. 4a), all numerical simulations show limited vertical settlements
227 outside the embankment area; however, Creep-SCLAY1S predicts more surface heaving in
228 this area, particularly in short-term. All three models provide good estimation of the surface
229 settlements shortly after construction (i.e., after 10 days). However, in long-term, MCC model
230 grossly underestimates the surface settlements; while S-CLAY1S provides an improved
231 prediction, although still underestimating the field data. The Creep-SCLAY1S model is able to
232 significantly better capture the field observations, while still underestimating the vertical
233 displacements after 5 and 10 years.

234 The numerical simulation results for the effect of PVD installation on the surface settlements,
235 up to a distance of 40 m from the centerline of the embankment, can be observed in Fig. 4b.
236 No field data is available for this side of the embankment; hence, the simulation results are
237 presented for the same times when measurements were taken for the other half of the
238 embankment. For all of the soil models, the predicted trends are almost the same as the case
239 without PVDs (see Fig. 4b). The predicted vertical settlement immediately after construction
240 remains very similar to the unimproved side of the embankment; however, for the longer time
241 periods the increased amounts of vertical settlements are apparent, in particular for when the
242 advanced models S-CLAY1S and Creep-SCLAY1S are used.

243 Estimation of the settlement influence zone is particularly important for planning the
244 construction work in urban areas with dense concentrations of buildings. The span of
245 settlement influence zone predicted by different models is different. For both sides of the
246 embankment the Creep-SCLAY1S model predicts a large influence zone (e.g., about 30 m
247 from the centerline of the embankment on the unimproved side), whereas MCC and S-
248 CLAY1S models clearly predict a smaller influence zone (e.g., up to about 16 m on the

249 unimproved side). From the figure, the extent of the influence zone seemingly decreases on
250 the side where the vertical drains are installed (see Fig. 4b), for example on this side MCC
251 and SCLAY1S predict an influence zone of less than 10 m and Creep-SCLAY1S predicts an
252 influence zone of less than 30 m.

253 **3.1.2.2 Lateral displacements**

254 For the unimproved side of the embankment, the lateral displacement predictions underneath
255 the crest (4 m from the centerline) of the embankment after 15 days, 1 year and 3 years of
256 consolidation, are presented in Fig. 5a and are compared with the field data. From the results,
257 MCC and S-CLAY1S evidently underestimate the lateral displacements of the soft soil deposit,
258 particularly at higher ground levels. Creep-SCLAY1S is able to accurately predict the
259 maximum value of lateral displacement under the crest; however, for deeper ground levels it
260 overestimates the deformations. This could be partly due to the approximating approach used
261 for the determination of the creep index. All three models are able to predict the depth at which
262 the maximum horizontal displacement occurs (2.5 m), with Creep-SCLAY1S providing more
263 representative predictions.

264 For the PVD improved side of the embankment, except for the top ground layer, all three
265 models provide reasonably good prediction of the lateral displacements under the
266 embankment crest in short-term (after 15 days consolidation) (Fig. 5b). The relatively large
267 displacement at the field near the ground surface is believed to be caused by error in the field
268 measurements. According to the field data, by comparing the measurements on both sides of
269 the embankment it appears that the installation of PVDs does not result in significant
270 differences on the amount of lateral displacements in short-term.

271 For the horizontal displacements at the toe of the embankment, generally all three models
272 provide reasonable predictions for the side of the embankment that is built on the unimproved
273 foundation soil (Fig. 6a). Overall, MCC and S-CLAY1S models underestimate the lateral
274 displacements at shallow depths, while Creep-SCLAY1S overestimates the horizontal
275 displacements a year after construction but provides more accurate predictions of lateral

276 displacements 3 years after construction. Better approximations of the lateral deformations at
277 deeper depths are obtained from the MCC and SCLAY1S models, while Creep-SCLAY1S
278 overestimates the lateral deformations at these depths.

279 With regards to the part of the embankment that is built on the PVD improved ground, all three
280 models fairly overestimate the amount of lateral displacements under the embankment toe
281 after 3 years of consolidation (Fig. 6b). This could be due to the fact that friction effects
282 between the soft soil and the PVDs are neglected in the numerical simulations. The narrowly
283 spaced PVDs are believed to act as some sort of “reinforcements” that can reduce the long-
284 term lateral displacements.

285 **3.1.2.3 Excess pore pressure**

286 Pneumatic piezometers were installed at different depths underneath the embankment to
287 monitor the excess PWP variations with time. Measurements are available only for the half of
288 the embankment built on the unimproved ground; however, the numerical simulation results
289 of the PWP dissipation are obtained for both sides of the embankment. Fig. 7a shows the *in-*
290 *situ* measurements of PWP related to piezometers located at a depth of 4 m, 7 m, 10 m, and
291 15 m under the centerline. The actual pore pressure measurements are rather erratic, not
292 following a regular trend, particularly for the depth of 4 m, therefore the field data should not
293 be assumed as definitive. The excess PWP initially builds up during the embankment
294 construction and then it is gradually dissipated with time. It is seen in Fig. 7a that all three
295 constitutive models overestimate the initial excess PWP build up at 4 m and 7 m depths.
296 However, a relatively accurate prediction of initial excess PWP is obtained at deeper depths
297 i.e. 10 m and 15 m.

298 Considering the plots of PWP dissipation with time in Fig. 7a, it is observed that the dissipation
299 rate is faster when the isotropic MCC and time-independent SCLAY1S models are used, while
300 the application of the Creep-SCLAY1S results in the slowest rate of excess PWP dissipation.
301 This trend is observed at all depths analyzed here. Note that at 10 m and 15 m depths, the

302 predictions of Creep-SCLAY1S show an increasing build-up of excess PWP up to day 650
303 (not shown here) from when the dissipation of excess PWP is commenced.

304 For the embankment side that was built on the PVD improved ground, all three models initially
305 show a sharp increase in the amount of excess PWP immediately after construction, followed
306 by a faster dissipation rate which is sensible as additional dissipation paths are provided by
307 the PVDs to discharge excess pore pressures (Fig. 7b). The results in Fig. 7 are presented for
308 the first 500 days of consolidation; however, the numerical analysis showed that when the
309 MCC model is used the excess PWP fully dissipated after 3500 days of consolidation, this is
310 the time that according to MCC consolidation settlement stops progressing. When S-CLAY1S
311 and Creep-SCLAY1S models are used the PWP dissipation prolongs into the following years
312 which is why with these models the consolidation settlement is continually progressing.

313 **3.1.2.4 Stress field and state parameters**

314 The installation of vertical drains also alters the stress field underneath the embankment. The
315 presence of drains leads to an increase in the stress values in the region near the drains, while
316 far from the drains the stress field approximately returns to that of the field underneath the
317 embankment without PVDs. This behavior has been observed for both vertical and horizontal
318 stresses; Fig. 8a shows the stress distribution along the embankment foundation 15 days after
319 construction and at a depth of 2.7 m, using the Creep-SCLAY1S model. The same behavior,
320 but with lower peaks at the drain locations, is observed for when several years of consolidation
321 have passed. Note that, due to the close spacing of PVDs, directly underneath the
322 embankment the effective mean stress values are continually increasing and decreasing.

323 Along with the stress field, column installation also influences the state parameters of the soil
324 such as void ratio. Void ratio decreases near the drains (see Fig. 8b) indicating a densification
325 of the soil due to fast drainage in this area. In between the drains, the value of the void ratio
326 increases, but it does not reach the values corresponding to when the foundation soft soil is
327 unimproved.

328 In a similar manner, the presence of PVDs influences the structure of the soil. Considering
329 destructuration parameter χ (Fig. 8c), the presence of drains causes a decrease of this state
330 parameter at the proximity of the drains, which is likely to be due to the disturbance caused
331 by the presence of the drain. The recovery in between the drains does not reach the values
332 of the simulation without PVDs.

333 **3.2 Matching techniques**

334 As discussed earlier, different matching techniques can be adopted to calculate the equivalent
335 permeability for the soil deposit when PVDs are installed. In this study the applications of two
336 different matching techniques are compared, one is a popular method proposed by [Hird et al.](#)
337 [\(1992\)](#) and the second is a less known method proposed by [Lin et al. \(2000\)](#). Considering the
338 parameters presented in Table 3, the equivalent permeability with the matching technique
339 proposed by [Lin et al. \(2000\)](#) is obtained as $k_{pl} = 0.012k_h$, which is a value very close to the
340 one obtained with the formulation of [Hird et al. \(1992\)](#).

341 Comparing the long-term settlement plots of the two sides of the case study embankment
342 studied in this paper (Fig. 9a) the numerical results obtained using the two matching
343 techniques are very similar. Also in terms of lateral deformations, the difference between the
344 results corresponding to the application of the two matching techniques is not noticeable (Fig.
345 9b). It is difficult to point out which is the more appropriate matching technique as the results
346 are almost identical.

347 When adopting the combined matching technique of [Hird et al. \(1992\)](#), one has to preselect
348 the value of the width of the equivalent plane-strain unit cell in order to obtain the
349 corresponding permeability, as the model takes into account both geometry and permeability
350 factors. By changing the value of B , in this instance for example adopting $B = 1$, the
351 permeability value changes accordingly ($k_{pl} = 0.0504k_h$). It is observed that greater spacing
352 between the drains leads to a remarkable increase in settlement predictions (Fig. 10a).
353 Distribution of the effective stress parameter is slightly influenced by increase in drain spacing,

354 resulting in lower decrease/increase of stresses within the PVD improved soil (Fig. 10b).
355 Variations of the state parameters e and χ are also decreased with increase in drain spacing
356 (Figs. 10c and d). In fact, higher values of equivalent plain-strain permeabilities obtained from
357 using higher drain spacing leads to a higher rate of consolidation and consequently higher
358 degradation of the inter-particle bonds (destruction) within the PVD improved area. The
359 recovery in between the drains does not reach the values of the simulation with $B = 0.5$. An
360 advantage of assuming a greater value of B is the possibility to better control the FE mesh,
361 adopting a less refined mesh, therefore increasing the efficiency of the simulation.

362 As in the formulation of the equivalent plain-strain permeability proposed by [Lin et al. \(2000\)](#)
363 the geometry of the model is not considered, adopting different values for the equivalent plane-
364 strain cell does not alter the predictions. This implies that no further simplification of the
365 numerical model is feasible when the matching technique of [Lin et al. \(2000\)](#) is used.
366 Therefore, adopting an equivalent plain-strain width ($2B$) equal to the drain spacing (S) is
367 necessary for modelling PVD improved soil foundations.

368 **4 Conclusions**

369 In this paper, the influence of prefabricated vertical drains (PVDs) installation on the
370 consolidation response of the soft soils is analyzed. A case study test embankment namely
371 Haarajoki embankment is taken into consideration. Three different soil constitutive models are
372 applied for the numerical simulations (MCC, S-CLAY1S and the newly developed Creep-
373 SCLAY1S) in order to highlight the importance of considering time-effects (i.e., creep) in
374 natural soil behavior at practical level.

375 Based on the results, the Creep-SCLAY1S model appeared to be capable of providing
376 reasonably accurate predictions of the delayed soft soil response in general, and the PVD
377 installation effects in particular. The inability of the MCC and S-CLAY1S models to reproduce
378 the delayed response of the clay makes these models noticeably unviable for modelling case
379 studies where the soil response is considerably prone to creep. Furthermore, given the

380 influence of the modified creep parameter values for accurate modelling of progressive
381 deformations with the Creep-SCLAY1S model, the good agreement between the creep model
382 predictions and observed settlements indicates that, where direct test data is not available,
383 the adopted methodology (i.e., $C_{\alpha i} = C_{\alpha} \lambda_i / \lambda$) for estimation of intrinsic creep index values is
384 reasonably reliable for practical applications.

385 Concerning the numerical results for lateral deformations (see Fig. 5) there are clear
386 discrepancies between model predictions and field data at the ground level which could be
387 due to errors during lateral deformation measurements at the surface of the ground.

388 From the results presented, it could be observed that embankment loading combined with
389 prefabricated vertical drains is a very effective ground improvement technique for soft soil
390 deposits. In fact, the installation of PVDs significantly accelerates the settlement of soft clays
391 and the process of excess pore pressure dissipation. In this way, the construction project can
392 proceed faster without further damaging settlements in subsequent years. Additionally, the
393 presence of vertical drains alters the stress field and the soil state parameters, leading to a
394 higher stress level in the PVD improved area as well as further densification of the soil.

395 The actual field condition around vertical drains is 3D; therefore, a comprehensive analysis of
396 an embankment built over a soil deposit with a large number of PVDs should be conducted
397 with a fully three dimensional numerical model. However, an appropriate matching technique
398 to convert the vertical drain system into equivalent plane-strain condition allows using a
399 representative 2D plane-strain model, which is computationally less expensive. Two different
400 matching techniques, proposed by [Hird et al. \(1992\)](#) and [Lin et al. \(2000\)](#), have been adopted
401 for the numerical simulations in this study, and it was observed that their application leads to
402 fairly similar results. Nevertheless, the matching technique proposed by [Hird et al. \(1992\)](#)
403 appears to be more versatile as it takes into account both geometry and permeability aspects,
404 and as such its application allows to better control the efficiency of the numerical simulation.

405 **References**

- 406 Abuel-Naga, H.M., Bergado, D.T., Gniel, J., 2015. Design chart for prefabricated vertical
407 drains improved ground. *Geotext. Geomemb.* 43, 537–546.
- 408 Berry, P. L., and Poskitt, T. J., 1972. The consolidation of peat. *Géotechnique* 22 (1), 27-52.
- 409 Brinkgreve R.B.J., Engin E., Swolfs W.M., 2014. *Plaxis 2014 reference manual*, Plaxis, Delft,
410 Netherlands.
- 411 Cascone, E., Biondi, G., 2013. A case study on soil settlements induced by preloading and
412 vertical drains. *Geotext. Geomemb.* 38, 51–67.
- 413 Chen, J.F., Tolooiyan, A., Xue, J.F., Shi, Z.M., 2016. Performance of a geogrid reinforced soil
414 wall on PVD drained multilayer soft soils. *Geotext. Geomemb.* 44 (3), 219–229.
- 415 Deng, Y.B., Xie, K.H., Lu, M.M., Tao, H.B., Liu, G.B., 2013. Consolidation by prefabricated
416 vertical drains considering the time dependent well resistance. *Geotext. Geomemb.* 36,
417 20–26.
- 418 Finnish National Road Administration, 1997. Competition to calculate settlements at the
419 Haarajoki test embankment. Competition programme, competition materials, Finnra,
420 Helsinki, Finland.
- 421 Grimstad, G., Abate, S., Nordal, S., Karstunen, M., 2010. Modeling creep and rate effects in
422 structured anisotropic soft clays. *Acta Geotechnica* 5, 69–81.
- 423 Hansbo, S., 1979. Consolidation of clay by band-shaped vertical drains. *Ground Eng.* 12 (5),
424 16–25.
- 425 Hird C.C., Pyrah I.C., Russell D., 1992. Finite element modeling of vertical drains beneath
426 embankments on soft ground. *Géotechnique* 42 (3). 499–511.
- 427 Hu, Y.Y., Zhou, W.H., Cai, Y.Q., 2014. Large-strain elastic viscoplastic consolidation analysis
428 of very soft clay layers with vertical drains under preloading. *Can. Geotech. J.* 51, 144–
429 157.

430 Indraratna, B., Sathananthan, I., Rujikiatkamjorn, C., Balasubramaniam A. S., 2005. Analytical
431 and numerical modelling of soft soil stabilized by PVD incorporating vacuum preloading.
432 Int. J. Geomech. 5 (2), 114–124.

433 Karstunen, M., Krenn, H., Wheeler, S. J., Koskinen, M., Zentar, R., 2005. The effect of
434 anisotropy and destructuration on the behaviour of Murro test embankment. Int. J.
435 Geomech. 5 (2), 87–97.

436 Karstunen, M., Rezaia, M., Sivasithamparam, N., Yin, Z-Y., 2015. Comparison of anisotropic
437 rate-dependent models for modeling consolidation of soft clays. Int. J. Geomech. 15 (5),
438 1–11.

439 Kim, Y.T., 2012. Strain rate-dependent consolidation behaviors of embankment with or without
440 vertical drains. Marine Georesour. Geotech. 30 (4), 274–290.

441 Kim, Y.T., Lee, S.R., 1997. An equivalent model and back-analysis technique for modelling in
442 situ consolidation behavior of drainage-installed soft deposits. Comp. Geotech. 20 (2),
443 125–142.

444 Lam, L.G., Bergado, D.T., Hino, T., 2015. PVD improvement of soft Bangkok Clay with and
445 without vacuum preloading using analytical and numerical analyses. Geotext.
446 Geomemb. 43, 547–557.

447 Leoni, M., Karstunen, M., and Vermeer, P.A., 2008. Anisotropic creep model for soft soils.
448 Géotechnique 58 (3), 215–226.

449 Lin D.G., Kim H.K., Balasubramaniam A.S., 2000. Numerical modelling of prefabricated
450 vertical drain. Geotech. Eng. J. of SEAGS 31 (2), 109–125.

451 Lo, S.R., Karim, M.R., Gnanendran, C.T., 2013. Consolidation and creep settlement of
452 embankment on soft clay: prediction versus observation. In: Geotechnical Predictions
453 and Practice in Dealing with Geohazards. Springer Netherlands, 77–94.

454 Mesri, G., Godlewski, P.M., 1977. Time and stress-compressibility interrelationship. J.
455 Geotech. Eng-ASCE 103 (5), 417–430.

456 Nguyen, T.T., Indraratna, B., 2017. Experimental and numerical investigations into hydraulic
457 behaviour of coir fibre drain. Can. Geotech. J. 54 (1), 75-87

458 Rezania, M., Sivasithamparam, N., and Mousavi-Nezhad, M., 2014. On the stress update
459 algorithm of an advanced critical state elasto-plastic model and the effect of yield
460 function equation. *Finite Elem. Anal. Des.* 90, 74-83.

461 Rezania, M., Taiebat, M. and Poletti, E., 2016a. A viscoplastic SANICLAY model for natural
462 soft soils. *Comp. Geotech.* 73, 128-141.

463 Rezania, M., Mousavi-Nezhad, M., Zanganeh, H., Castro, J., Sivasithamparam, N., 2016b.
464 Modelling pile setup in natural clay deposit considering soil anisotropy, structure, and
465 creep effects: Case study. *Int. J. Geomech.* 04016075, 1–13.

466 Roscoe, K.H., Burland, J.B., 1968. On the generalized stress-strain behaviour of 'wet' clay.
467 *Engineering plasticity*, Cambridge University Press, Cambridge, U.K. 553–609.

468 Rowe, R.K., Taechakumthorn, C., 2008. Combined effect of PVDs and reinforcement on
469 embankments over rate-sensitive soils. *Geotext. Geomemb.* 26, 239–249.

470 Wheeler, S.J., Näätänen, A., Karstunen, M., Lojander, M., 2003. An anisotropic elastoplastic
471 model for soft clays. *Can. Geotech. J.* 40, 403–418.

472 Sivasithamparam, N., Karstunen M., Bonnier, P., 2015. Modelling creep behaviour of
473 anisotropic soft soils. *Comp. Geotech.* 69, 46–57.

474 Wang, J., Cai, Y. Ma, J., Chu, J., Fu, H., Wang, P., Jin, Y., 2016. Improved vacuum preloading
475 method for consolidation of dredged clay-slurry fill. *J. Geotech. Geoenviron. Eng.*
476 06016012, 1–5.

477 Xiao, D.P., 2001. Consolidation of soft clay using vertical drains. Ph.D. Thesis, Nanyang
478 Technological University, Singapore.

479 Xue, J-F., Chen, J-F., Liu, J-X. , Shi, Z-M., 2014. Instability of a geogrid reinforced soil wall on
480 thick soft Shanghai clay with prefabricated vertical drains: A case study. *Geotext.*
481 *Geomemb.* 42, 302–311.

482 Yildiz, A., Karstunen, M., and Krenn, H., 2009. Effect of anisotropy and destructuration on
483 behaviour of Haarojoki test embankment. *Int. J. Geomech.* 153–165.

484 Zhu, G. and Yin, J.H., 2000. Finite element consolidation analysis of soils with vertical drain.
485 Int. J. Numer. Anal. Met. 24 (4), 337–366.
486

487 **List of notations**

B	Half width of plane-strain unit cell	α_0	Initial value of anisotropy
c'	Cohesion	α	Scalar value of anisotropy
c_k	Permeability change index	β	Creep exponent
c_α	Creep index	χ	Bonding parameter
$c_{\alpha i}$	Intrinsic creep index	χ_0	Initial value of bonding parameter
D	Equivalent diameter of unit cell	γ	Unit weight
D_m	Equivalent diameter of mandrel	κ	Slope of swelling/recompression line from $e - \ln p_0$ diagram
D_s	Equivalent diameter of smear zone	κ^*	Modified slope of swelling/recompression line from $e - \ln p_0$ diagram
D_w	Equivalent diameter of drain	λ	Slope of post yield compression line from $e - \ln p_0$ diagram
E	Young's modulus	λ_i	Slope of intrinsic post yield compression line from $e - \ln p_0$ diagram
e_0	Initial void ratio	λ^*	Modified slope of post yield compression line from $e - \ln p_0$ diagram
e	Void ratio	λ_i^*	Modified slope of intrinsic post yield compression line from $e - \ln p_0$ diagram
K_0	coefficient of lateral earth pressure at rest	μ^*	Modified creep index
k	Permeability	μ_i^*	Intrinsic modified creep index
k_h	Horizontal permeability of undisturbed soil	ω	Rate of rotation
k_{hpl}	Equivalent plane-strain horizontal permeability	ω_d	Rate of rotation due to deviator stress
k_s	Horizontal permeability of smear zone	ζ	Parameter controlling absolute rate of destructuration
k_v	Vertical permeability of undisturbed soil	ζ_d	Parameter controlling relative effectiveness of destructuration rate
M	Stress ratio at critical state	ν	Poisson's coefficient
R	Equivalent radius of unit cell	ϕ'	Friction angle
R_s	Equivalent radius of smear zone	τ	Reference time
R_w	Equivalent radius of drain	NCS	Normal consolidation surface
S	Drain spacing	POP	Pre-overburden pressure

488

489

490

491

Table 1 – Model constants adopted for Haarajoki clay layers

Type	Parameter	Layer 1a (0-1m)	Layer 1b (1-2m)	Layer 2 (2-6m)	Layer 3 (6-7m)	Layer 4 (7-12m)	Layer 5 (12-15m)	Layer 6 (15-18m)	Layer 7 (18-22.2m)
Initial stress state	e_0	1.25	1.25	2.90	2.60	2.35	2.20	2.00	1.25
	γ (kN/m^3)	17.5	17.5	14.3	14.3	15.1	15.1	15.7	17.5
	POP (kN/m^2)	110	32	32	32	32	32	32	32
Elasticity	ν	0.2	0.2	0.2	0.2	0.2	0.2	0.2	0.2
	κ	-----	0.010	0.010	0.030	0.036	0.030	0.034	0.004
Critical State	M	-----	1.60	1.15	1.43	1.15	1.20	1.55	1.55
	λ	-----	0.20	1.33	0.96	0.96	1.06	0.45	0.10
	λ_i	-----	0.20	0.38	0.27	0.26	0.30	0.13	0.03
Anisotropic	α_0	-----	0.63	0.44	0.55	0.44	0.46	0.61	0.61
	ω	-----	37	33	49	44	35	36	37
	ω_d	-----	1.02	0.70	0.97	0.70	0.76	1.01	1.01
Destructuration	χ_0	-----	4	22	30	45	45	45	45
	ζ	-----	8	8	8	8	8	8	8
	ζ_d	-----	0.2	0.2	0.2	0.2	0.2	0.2	0.2
Viscosity	μ^*	-----	1.16E-3	4.44E-3	3.47E-3	3.73E-3	4.32E-3	1.95E-3	5.79E-3
Permeability	k_h (m/d)	3.46E-4	3.46E-4	1.04E-4	8.64E-5	8.64E-5	8.64E-5	8.64E-5	3.46E-4
	k_v (m/d)	1.73E-4	1.73E-4	5.18E-5	4.32E-5	4.32E-5	4.32E-5	4.32E-5	1.73E-4
	c_k	0.45	0.45	1.12	1.29	0.74	0.61	0.40	0.40

492

493

494

Table 2 – Parameters adopted for matching technique

S [m]	B [m]	R [m]	R_s [m]	R_w [m]	R_s/R_w	k_h/k_s
1	0.5	0.564	0.268	0.034	8	20

495

496

497

Table 3 – Modified coefficients of permeability according to the matching techniques

Layer	Layer 1a (0-1m)	Layer 1b (1-2m)	Layer 2 (2-6m)	Layer 3 (6-7m)	Layer 4 (7-12m)	Layer 5 (12-15m)	Layer 6 (15-18m)	Layer 7 (18-22.2m)
k_{hpl} (Hird et al. 1992)	4.36E-6	1.31E-6	1.09E-6	1.09E-6	1.09E-6	1.09E-6	1.09E-6	4.36E-6
k_{hpl} (Lin et al., 2000)	4.15E-6	1.25E-6	1.04E-6	1.04E-6	1.04E-6	1.04E-6	1.04E-6	4.15E-6

498

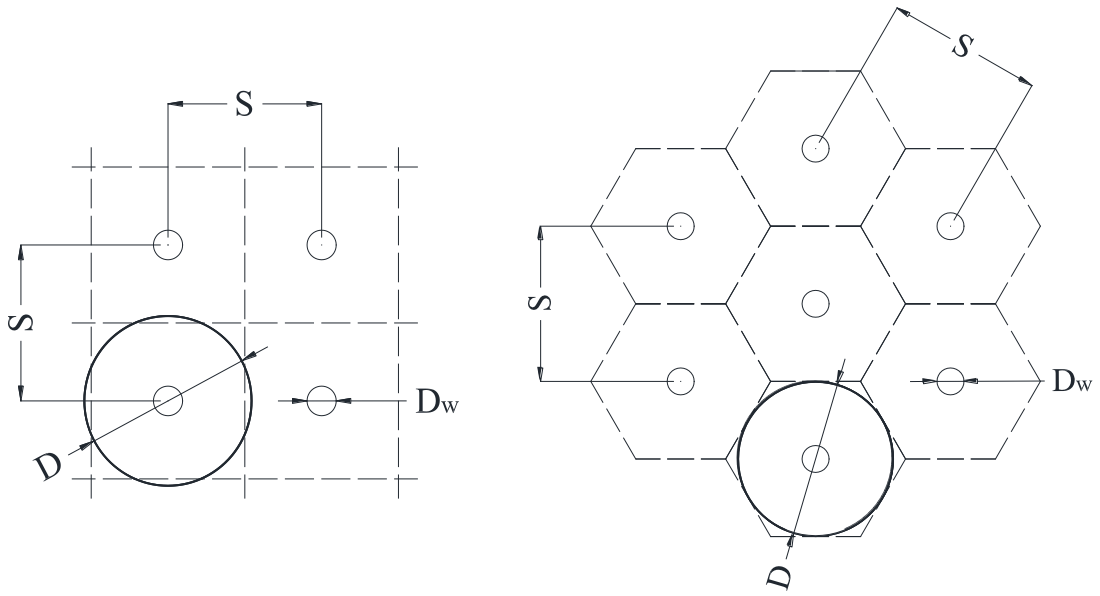
499

500

501

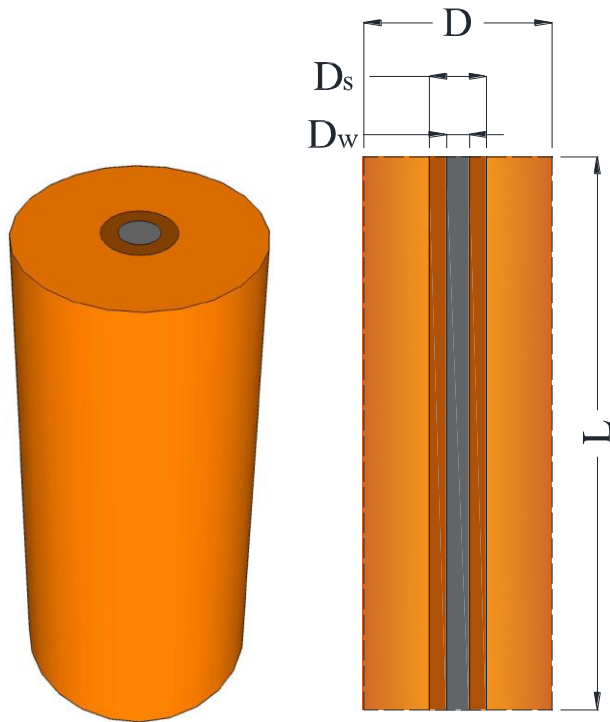
502

503



(a)

(b)



(c)

504

Fig. 1. PVD pattern: (a) square pattern; (b) triangular pattern; (c) drain with smear zone

505

506

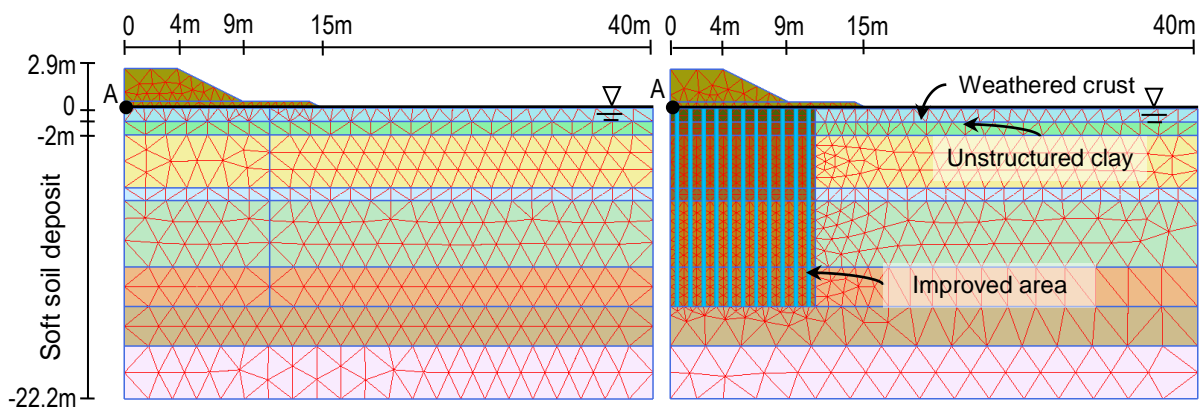
507

508

509

510

511



512

513 Fig. 2. Geometry of the finite element models adopted for the simulation of Haarajoki test embankment and the

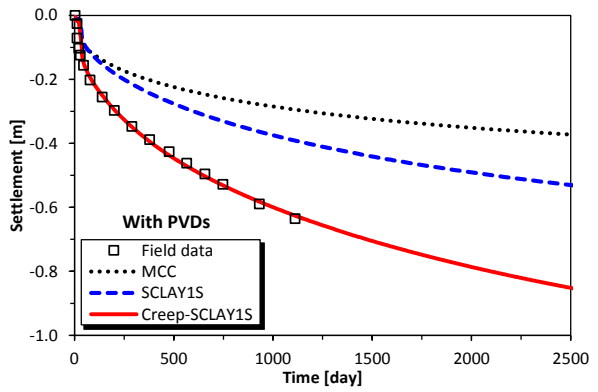
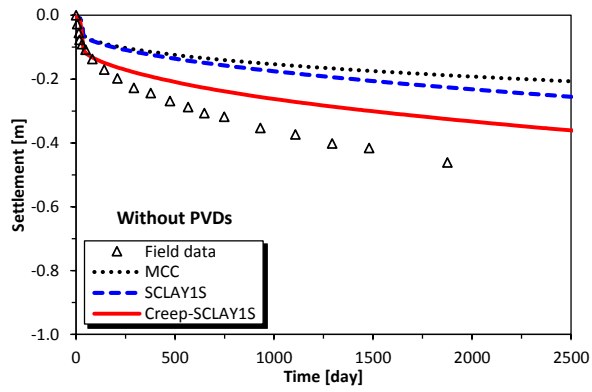
514 position of PVDs; Left: unimproved side; Right: improved side of the foundation soil

515

516

517

518



519

(a)

(b)

520

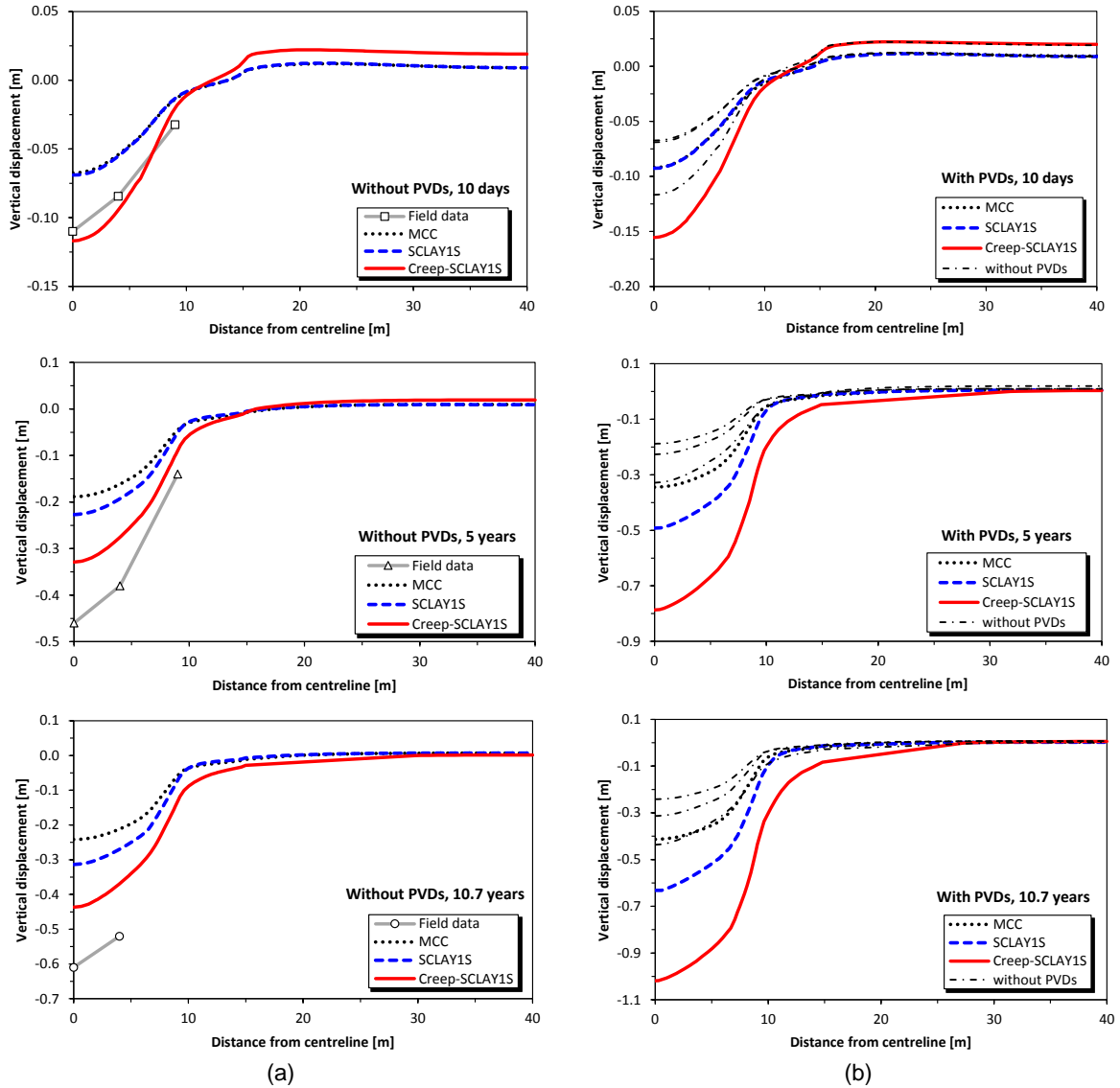
Fig. 3. Time- settlements plots for Haarajoki embankment at centreline: (a) without PVDs; (b) with PVDs

521

522

523

524



525

Fig. 4. Surface settlement throughs for Haarajoki embankment: (a) without PVDs; (b) with PVDs

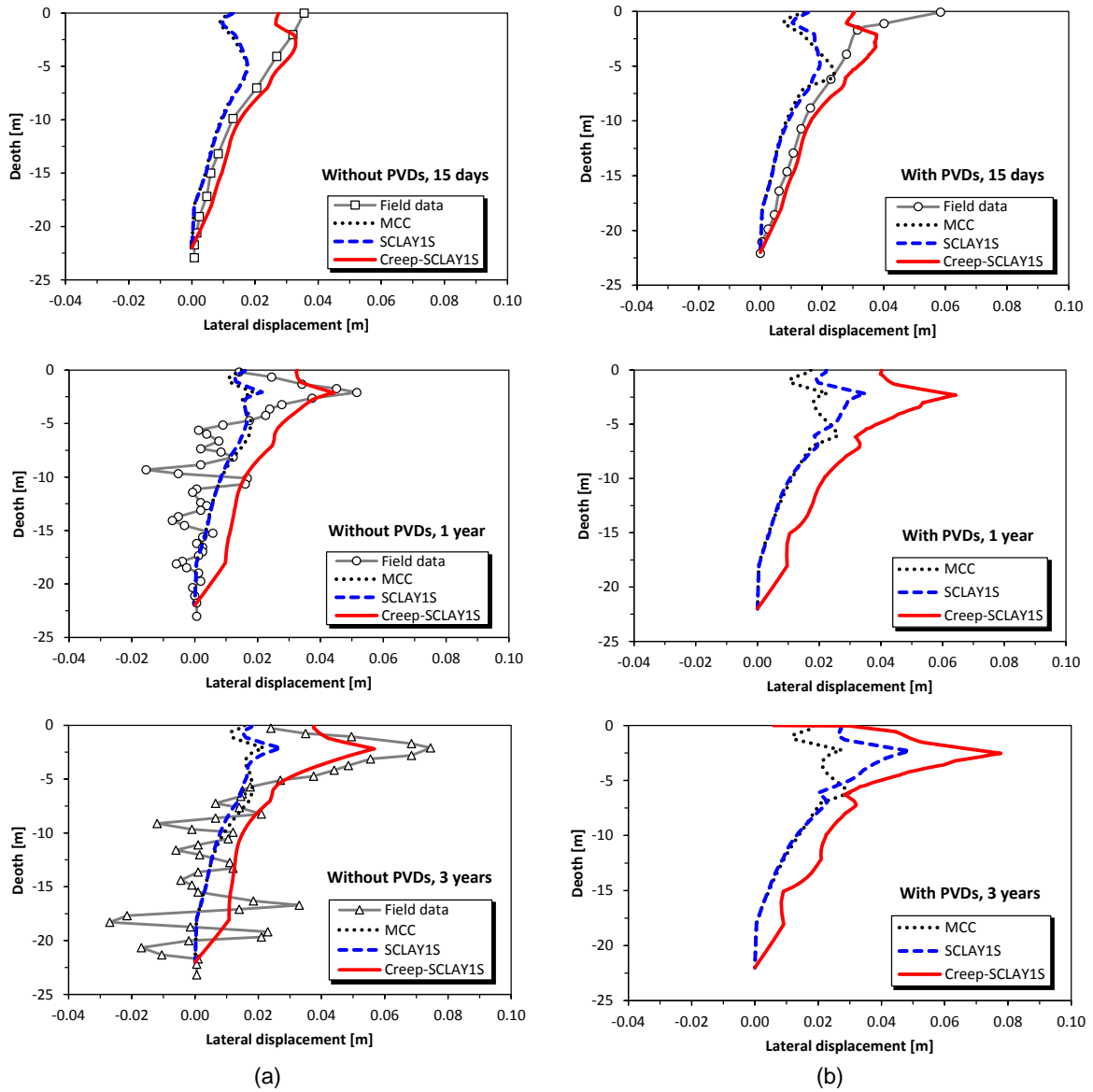
526

527

528

529

530



531

Fig. 5. Lateral displacement predictions for Haarajoki embankment under the crest: (a) without PVDs (b) with

532

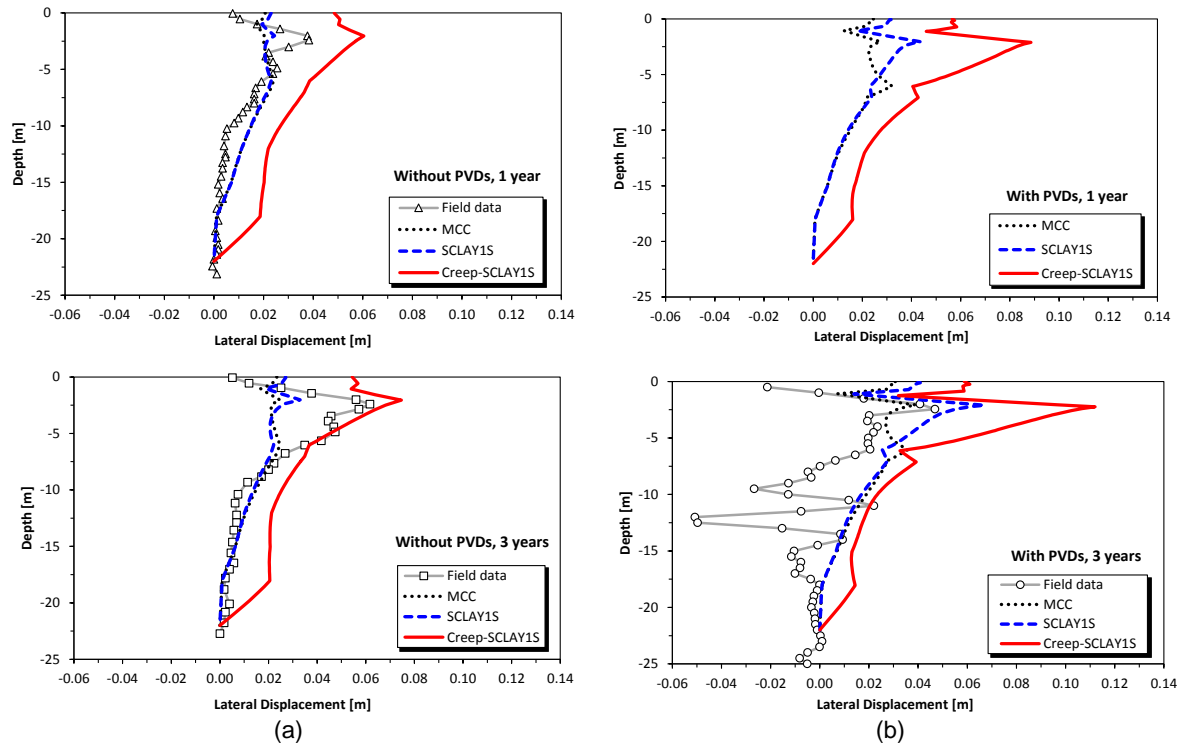
PVDs

533

534

535

536



537

Fig. 6. Lateral displacements predictions for Haarajoki embankment under the toe: (a) without PVDs; (b) with

538

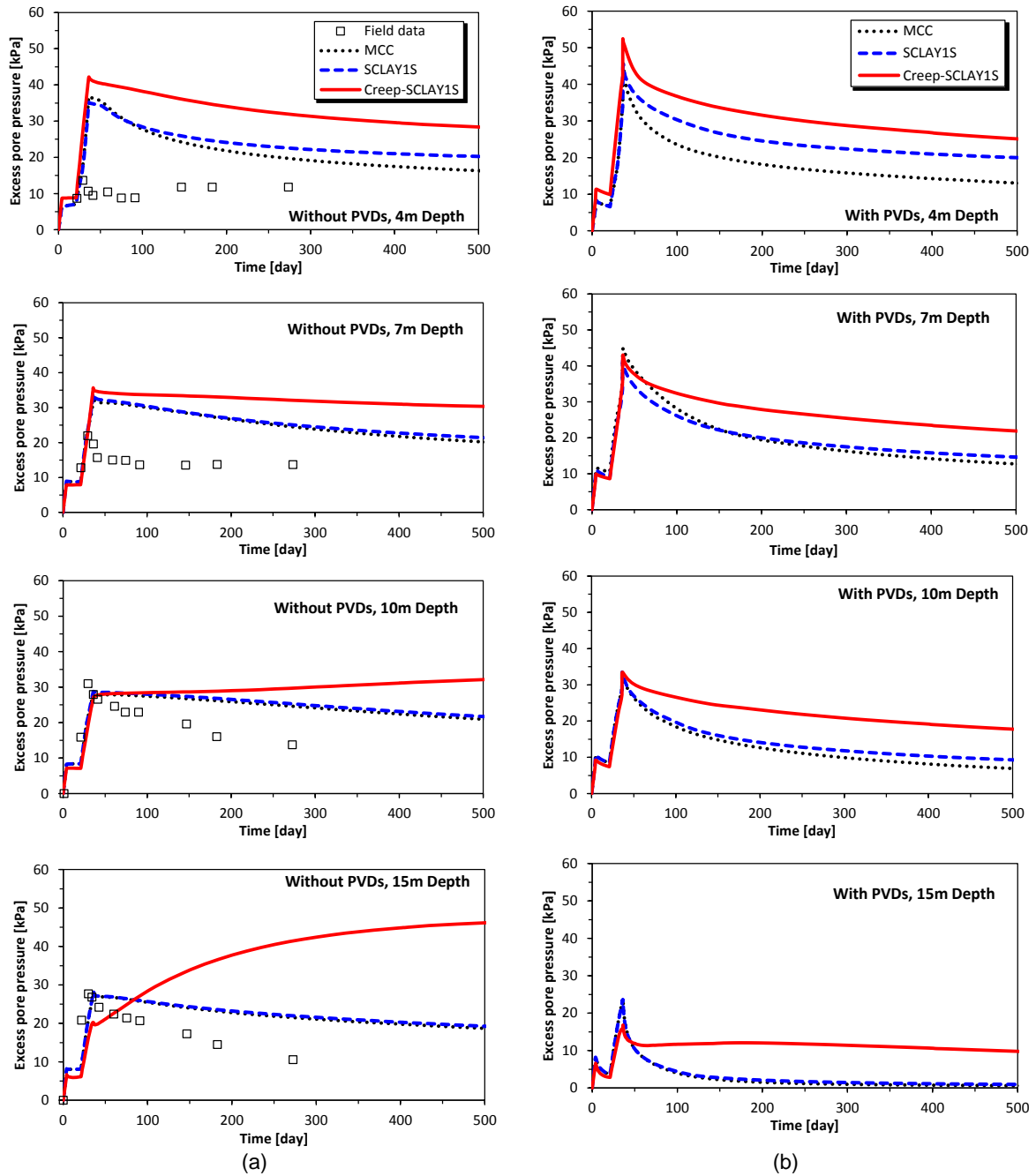
PVDs

539

540

541

542

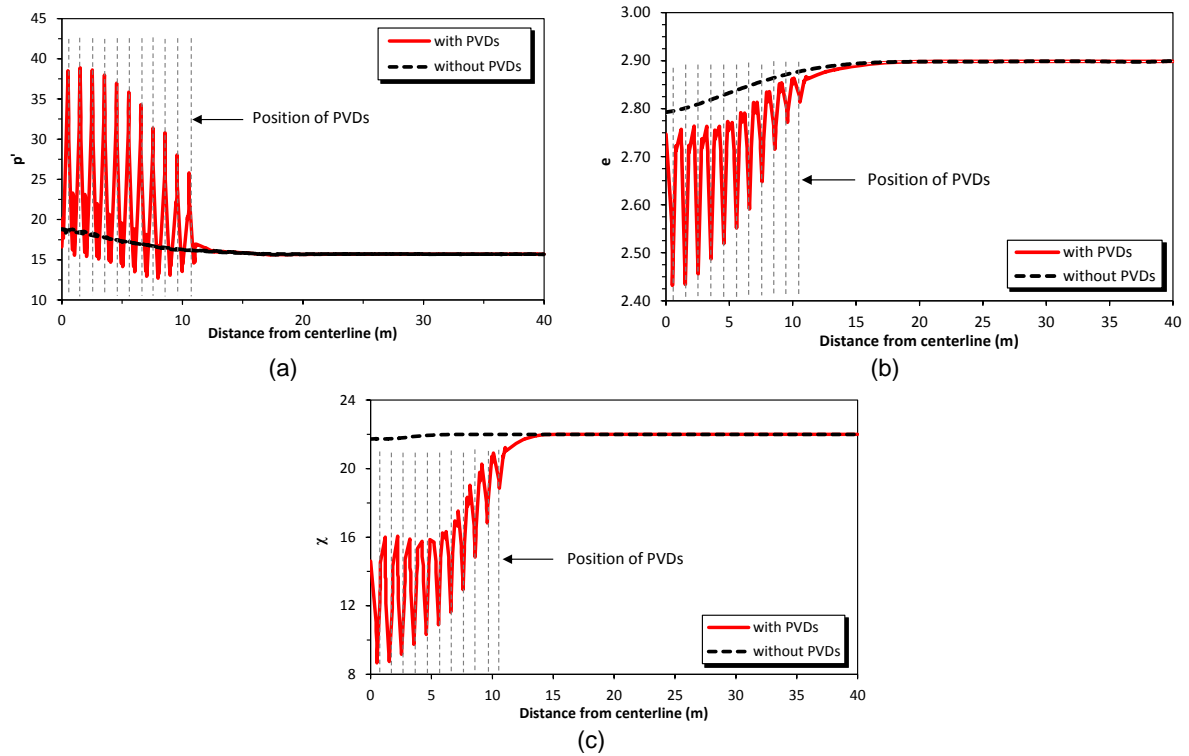


543

Fig. 7. Excess pore water pressure dissipation with time at different depths: (a) without PVDs; (b) with PVDs

544

545



546 Fig. 8. Effect of installation of vertical drains: (a) effective mean stress distribution 15 days after construction; (b)

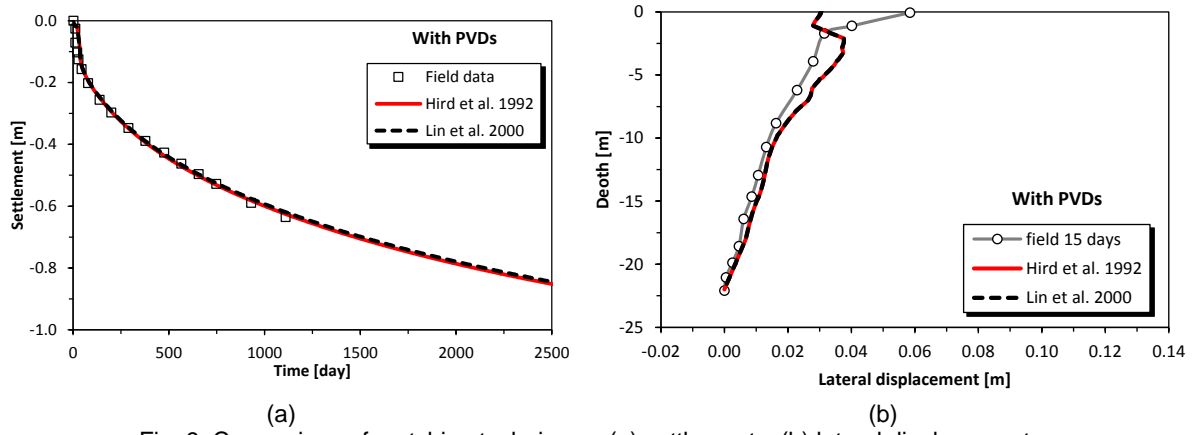
547 void ratio distribution 1 year after construction; (c) bonding parameter distribution 1 year after construction

548

549

550

551



(a)

(b)

552

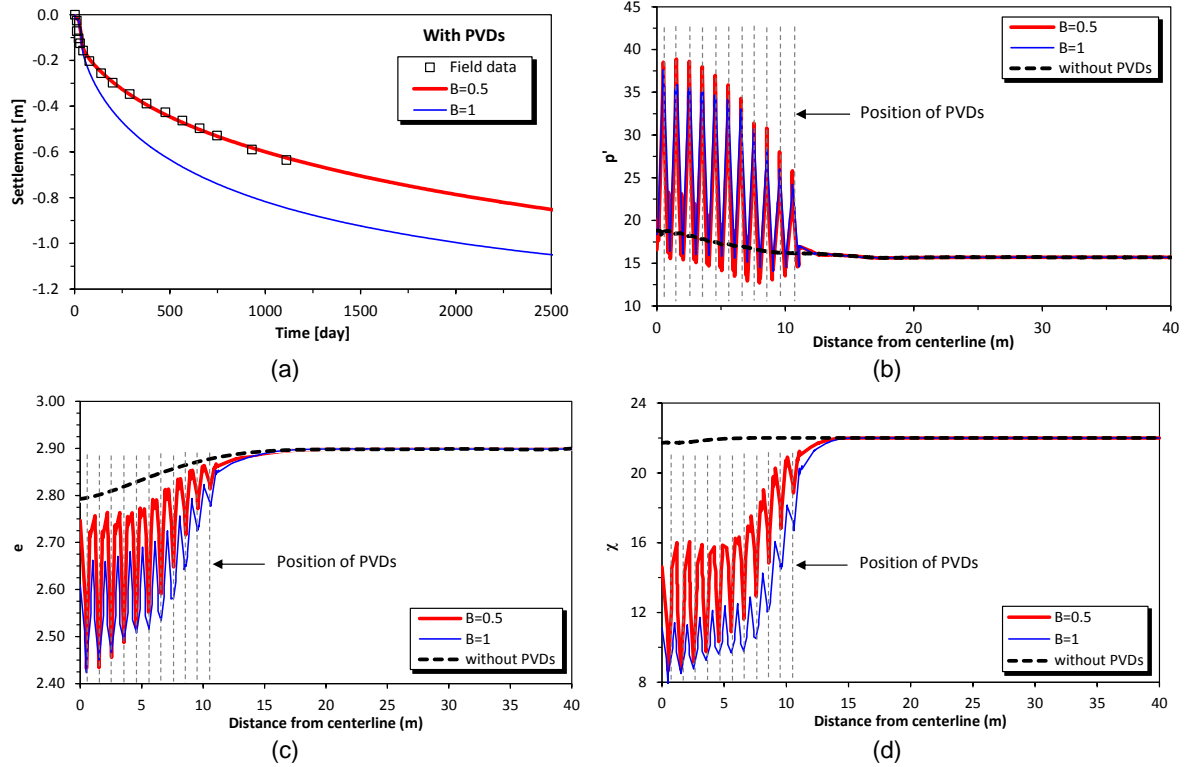
Fig. 9. Comparison of matching techniques: (a) settlements; (b) lateral displacements

553

554

555

556



557

Fig. 10. Influence of equivalent plane-strain width of the unit cell: (a) settlements; (b) mean effective stress; (c)

558

void ratio; (d) bonding parameter

559